INTERNATIONAL GEOLOGY REVIEW, 2017
VOL. 59, NO. 13, 1621–1631
https://doi.org/10.1080/00206814.2016.1213142

Relict chromian spinels in Tulu Dimtu serpentinites and listvenite, Western Ethiopia: implications for the timing of listvenite formation

Ayano Sofiya [a,b,c*], Akira Ishiwatari [d], Naoto Hirano [b] and Tatsuki Tsujimori [b]

[a]Department of Earth Science, Graduate School of Science, Tohoku University, Sendai, Japan; [b]Center for Northeast Asian Studies, Tohoku University, Sendai, Japan; [c]Department of Mineral Exploration, Geological Survey of Ethiopia, Addis Ababa, Ethiopia; [d]Nuclear Regulation Authority, Tokyo, Japan

ABSTRACT
Serpentinites (massive and schistose) and listvenite occur as tectonic sheets and lenses within a calcareous metasedimentary mélange of the Tulu Dimtu, western Ethiopia. The massive serpentinite contains high-magnesian metamorphic olivine (forsterite [fo] ~96 mol%) and rare relict primary mantle olivine ($Fo_{90–93}$). Both massive and schistose serpentinites contain zoned chromian spinel; the cores with the ferritchromite rims preserve a pristine Cr/(Cr+Al) atomic ratio (Cr# = 0.79–0.87), suggesting a highly depleted residual mantle peridotite, likely formed in a suprasubduction zone setting. Listvenite associated with serpentinites of smaller ultramafic lenses also contain relict chromian spinel having identical Cr# to those observed in serpentinites. However, the relict chromian spinel in listvenite has significantly higher $Mg/(Mg+Fe^{2+})$ atomic ratios. This suggests that a nearly complete metasomatic replacement of ultramafic rocks by magnesite, talc, and quartz to prevent $Mg–Fe^{2+}$ redistribution between relict chromian spinel and the host, that is, listvenite formation, took place prior to re-equilibration between chromian spinel and the surrounding mafic minerals in serpentinites. Considering together with the regional geological context, low-temperature CO_2-rich hydrothermal fluids would have infiltrated into ultramafic rocks from host calcareous sedimentary rocks at a shallow level of accretionary prism before a continental collision to form the East African Orogen (EAO).

ARTICLE HISTORY
Received 30 May 2016
Accepted 12 July 2016

KEYWORDS
Listvenite; carbonate metasomatism; serpentinization; East African Orogen; Ethiopia

1. Introduction

The East African Orogen (EAO) along eastern Africa and western Arabia is the world's largest Neoproterozoic to Cambrian orogenic belt (e.g. Stern 1993, 1994; Fritz *et al*. 2013). This amalgamated belt with an ~6,000 km length reflects collision of arcs or microcontinents against the Archaean Craton margins. The northern part of the EAO is dominated by metavolcano–sedimentary sequences with minor ophiolites. Although the palaeo-oceanic lithosphere and its metasomatic equivalent are minor components in EAO, those rocks contain key evidences to better understand the petrotectonic evolution, particularly the geodynamic processes enclosed in the building of the West Gondwana margin prior to the continental collision to form the EAO.

Understanding the metasomatic processes associated with ultramafic rocks is of considerable importance as emphasized by recent works on the formation of high-pressure/low-temperature vein-related rocks such as jadeitites (Sorensen *et al*. 2010; Harlow *et al*. 2015), as well as low-pressure/low-temperature fluid–rock interaction during listvenite formation (Hansen *et al*. 2005; Tsikouras *et al*. 2006; Aftabi and Zarrinkoub 2013; Boedo *et al*. 2015; Falk and Kelemen 2015). In Tulu Dimtu area in Western Ethiopia of the Arabian–Nubian Shield (ANS), carbonate-bearing serpentinites and listvenite occur as tectonic sheets and lenses in calcareous metasedimentary mélange (Figures 1 and 2). The listvenite is an unusual type of metasomatic, silica–carbonate rock formed by the carbonation of ultramafic rocks at low temperature (e.g. Halls and Zhao 1995). Although intense serpentinization and silica–carbonate metasomatism erased almost all the primary petrological characteristics of the original mantle peridotite in Tulu Dimtu, our petrological study confirmed the preservation of relict mantle olivine in serpentinite and relict chromian spinel in both serpentinite and listvenite. We

CONTACT Ayano Sofiya saay_2008@yahoo.com Department of Earth Science, Graduate School of Science, Tohoku University, 6-3 Aramaki Aza-Aoba, Aoba-ku, Sendai, Miyagi 980-8578, Japan
*Present address: Department of Earth Science, Graduate school of Science, Tohoku University, Aoba-ku, Sendai, Miyagi 980-8578, Japan
This article is part of the Special Issue entitled 'Petrotectonic and geochemical researches on subduction zones—A celebration of the career of Sorena S. Sorensen'.

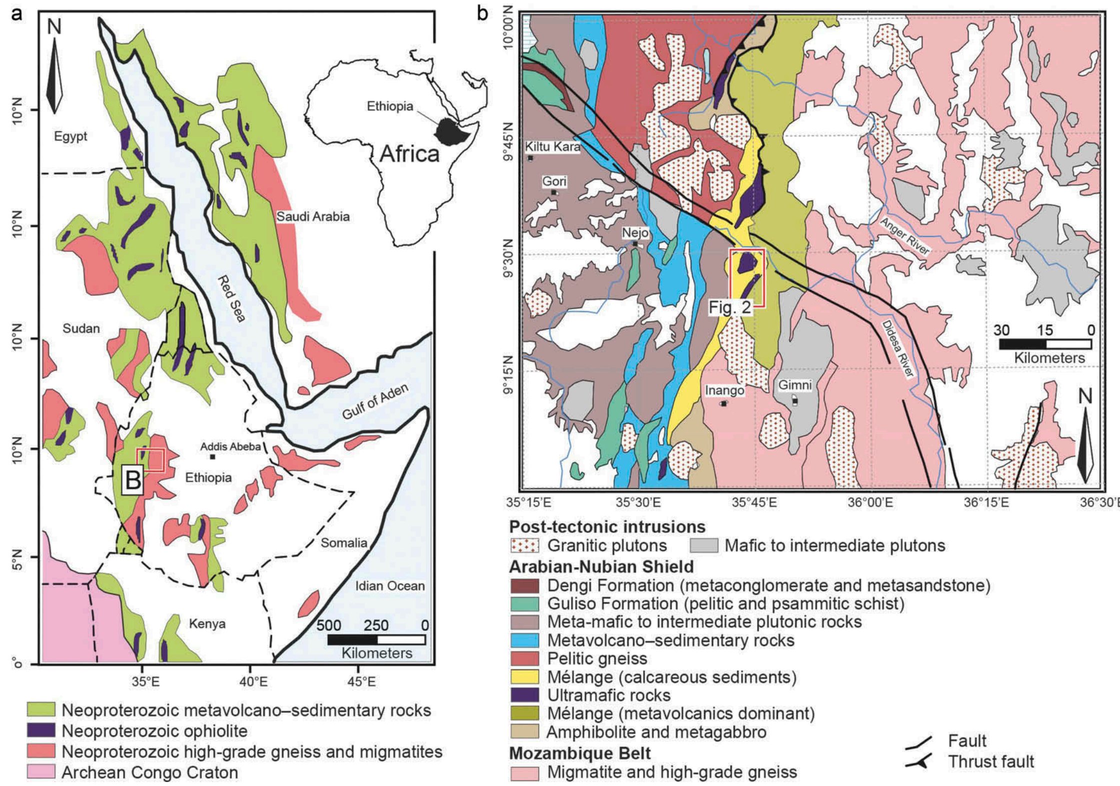

Figure 1. (a) Location map of the Arabian–Nubian Shield ophiolites (modified after Abdelsalam and Stern 1996) is also shown. (b) Generalized geological map of the Nekemte–Gimbi–Nejo region of Western Ethiopia showing the major geotectonic units.

consider that relict chromian spinel in listvenite can constrain a relative timing of carbonate metasomatism. In this contribution, we first report relict chromian spinels in serpentinites and listvenite in Tulu Dimtu, and discuss the listvenite-forming metasomatism.

2. Geological outline

2.1. Overview

Western Ethiopia, in general, is composed of rocks ranging in age from Precambrian to Tertiary. The Precambrian basement terrain of the East African orogenic system in Western Ethiopia consists of two geotectonic domains: (1) metamorphosed volcano-sedimentary rocks, meta-plutonic rocks, and related mélange with dismembered ophiolites of the ANS, and (2) high-grade gneisses/migmatites of the Mozambique Belt (MB) (Figure 1(a)). Stern (1993, 1994) coined the term EAO to encompass both the ANS and the MB. The EAO is a sequence of rocks with an age span of 950–450 Ma orogenic cycle (Kröner 1984). According to earlier authors (e.g. Ayalew *et al*. 1990; Kebede *et al*. 2001; Grenne *et al*. 2003), all basement rock units were intruded by post-tectonic intrusions; they were generated from suprasubduction to intraplate magmas (Ayalew *et al*. 1989; Kebede *et al*. 1999; Grenne *et al*. 2003).

Tectonic evolution of the Western Ethiopia basement recently reviewed by Tadesse and Tsegaye (2007) started with an E–W to NNW shortening, in which metasedimentary units with ultramafic rocks and syn- to pretectonic plutons were thrusted, folded, and sheared. This shortening produced original NNE–SSW-trending penetrative foliations. Progressive regional folding and locally discrete sinistral shearing steepened, which refolded the earlier structural elements in the later stages. The last deformation event, associated with brittle-ductile strike–slip faults, was an E–W shearing with considerable lateral displacement.

2.2. Ultramafic rocks in Tulu Dimtu area

In Western Ethiopia, the metavolcano–sedimentary unit with ultramafic rocks of the ANS is sandwiched between the high-grade gneiss/migmatite unit to the east and the west (Kazmin 1972; Kazmin *et al*. 1978; Tefera *et al*. 1996; Alemu and Abebe 2000). Aligned but discontinuous bodies of ultramafic rocks exposed along strike–slip shear and thrust zones have been interpreted as dismembered ophiolite (e.g. Kazmin 1976; de Wit and Chewaka

1981; Tadesse and Allen 2005). The ultramafic bodies occur in several localities of the Nekemte–Gimbi–Nejo region (Figure 1(b)). Those bodies were considered as dismembered fragments of the oceanic lithosphere, preserved as detached ophiolite allochthon within a back-arc continental marginal setting (Tadesse and Tsegaye 2007). Similar to other ophiolite bodies, they have experienced later continental collision and tectonic shortening (Stern *et al*. 2004).

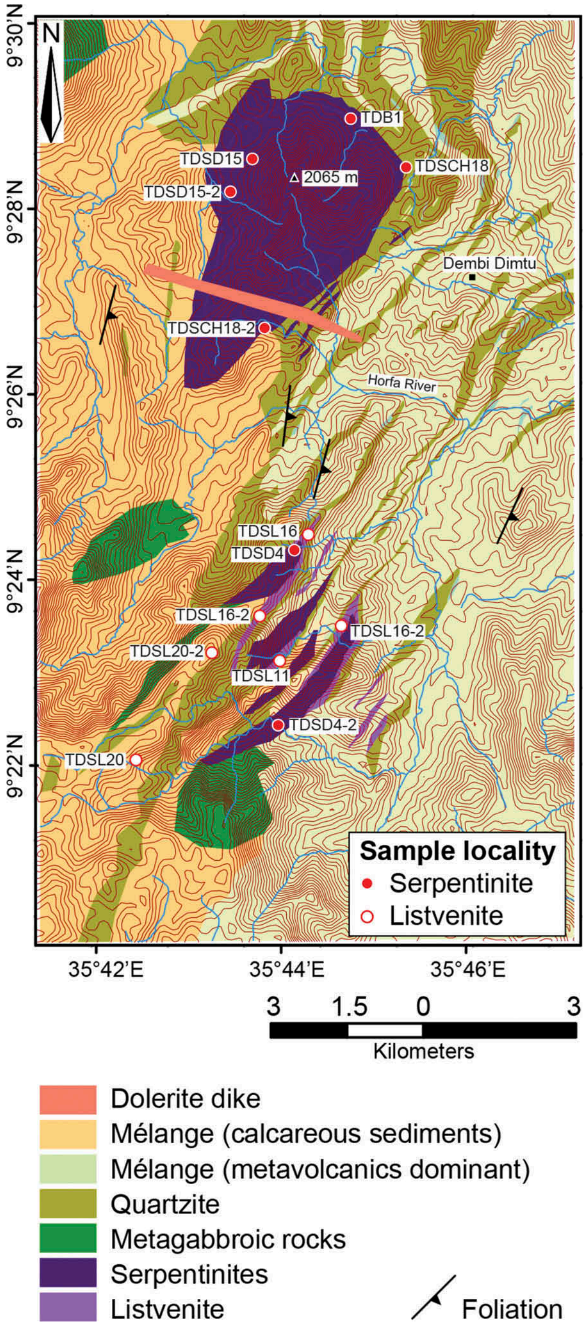

Figure 2. Geological map of Tulu Dimtu area showing sample locations.

Ultramafic rocks in the Tulu Dimtu area occur as tectonic sheets and lenses within a metasedimentary mélange. The largest body has a size of about 4 × 7 km (Figure 2). The metasedimentary mélange, including ultramafic rocks, is intruded by a post-tectonic dolerite (Figure 2). The ultramafic bodies comprise massive and schistose serpentinites, and small bodies accompany abundant listvenite. The margin of the bodies is highly sheared and schistose; the massive serpentinites are also locally sheared. Although the direct contact is not exposed, the occurrence of listvenites is common along the boundary zones between smaller ultramafic bodies and host metasedimentary rocks. Listvenites are also schistose, suggesting that the deformation in listvenite and schistose serpentinite was coeval. This infers that schistosities in schistose serpentinite and listvenite have developed after the listvenite formation. Listvenite in this area has been described as birbirite (de Wit *et al*. 1978; Alemu and Abebe 2000) (Figure 3). However, to date no petrological and geochemical studies have been conducted.

3. Analytical method

Concentrations of major (Si, Ti, Al, Fe, Mn, Mg, Ca, Na, K, and P) and trace (Ni, Cr, Rb, Ba, Nb, Sr, Zr, Y, and V) elements were analysed by a Rigaku RIX 2100 X-ray fluorescence spectrometer with an Rh tube at Tohoku University. The operating conditions for both major and trace elements were 50 kV accelerating voltage and 50 mA beam current. Results of these analyses are provided in Table 1.

Polished thin-sections were observed using a JEOL JSM-5410 scanning electron microscope (SEM) equipped with an Oxford Link ISIS energy-dispersive X-ray microanalysis system at Tohoku University. Back-

Figure 3. Photograph of a representative hand specimen of the investigated listvenite (sample TDSL-16).

Table 1. Bulk-rock compositions of massive serpentinites, schistose serpentinites, and listvenite.

Rock type	Massive serpentinite			Schistose serp.		Listvenite		
Sample	TDSD15	TDSD4	TDSD4-2	TDSCH18	TDSCH18-2	TDSL11	TDSL16	TDSL20
Major-element compositions (in wt.%)								
SiO_2	39.05	38.35	39.06	36.60	33.25	32.69	31.98	36.75
TiO_2	0.00	0.01	0.01	0.01	0.01	0.00	0.00	0.02
Al_2O_3	0.11	0.08	0.07	0.09	0.09	0.06	0.13	0.35
FeO*	7.45	7.93	7.38	6.60	6.94	5.83	7.01	6.79
MnO	0.11	0.09	0.09	0.11	0.12	0.08	0.11	0.07
MgO	40.96	37.28	38.48	37.65	36.68	35.73	36.15	35.00
CaO	0.19	0.01	0.01	0.08	0.07	0.05	0.10	0.03
Na_2O	n.d.	n.d.	n.d.	n.d.	n.d.	n.d.	n.d.	n.d.
K_2O	n.d.	n.d.	n.d.	n.d.	n.d.	n.d.	n.d.	n.d.
P_2O_5	<0.01	<0.01	<0.01	<0.01	<0.01	<0.01	<0.01	<0.01
LOI	12.49	11.36	11.45	17.52	20.22	23.93	23.29	19.65
Total	100.36	95.11	96.55	98.66	97.38	98.37	98.77	98.66
Trace-element compositions (μg/g)								
V	39.7	25	25.6	57.5	49.2	34.5	39.4	29.7
Cr	4471	5124	3455	8388	8923	6727	6151	3322
Ni	2359	2118	2214	2183	2277	2097	2146	2040
Rb	<0.1	<0.1	n.d.	0.6	0.4	n.d.	n.d.	0.5
Sr	2.7	3.2	2.1	5.6	4.1	3.4	3.3	3.3
Ba	n.d.	n.d.	n.d.	n.d.	n.d.	n.d.	n.d.	0.8
Y	n.d.	0.3	1.4	1.2	0.8	0.3	0.8	0.4
Zr	1.9	1.3	1.9	1.7	1.1	2.3	1.7	1.7
Nb	1.2	1.1	1.3	1.1	1.4	0.9	1.1	1.1

*Total Fe as FeO; n.d., not detected; LOI, loss of ignition.

scattered electron (BSE) microscopic imaging was performed at a 15 kV accelerating voltage and 1 nA beam current. Electron microscope quantitative analyses of rock-forming minerals were performed with a 15 kV accelerating voltage, 1 nA beam current, and <3 μm beam size. The oxide ZAF method was employed for matrix corrections. Representative analyses of olivine and chromian spinel are provided in Table 2.

4. Petrography

4.1. Serpentinite

Serpentinites of the Tulu Dimtu area can be divided into massive serpentinite (samples TDSD-4, TDSD-4–2, TDSD-15, and TDSD-15–2) and schistose serpentinite (TDB-1 and TDSCH-18) (Figure 4(a–c)). The massive serpentinite consists mainly of antigorite and magnesite with trace amounts of olivine (both primary and metamorphic), chromian spinel, talc, chlorite, and magnetite. Rare mesh texture after olivine and bastite pseudomorphs after orthopyroxene are observed. Some metamorphic olivine can be distinguished from relict by the presence of tiny magnetite inclusions. The schistose serpentinite is composed of antigorite and magnesite, with minor magnetite and chromian spinel. A penetrative schistosity is defined by the preferred orientation of antigorite.

Chromian spinel in both massive and schistose serpentinites occurs commonly as subhedral to anhedral, and exhibits a partial replacement texture, where the brownish pristine cores are rimmed by opaque ferritchromite. Some grains are fractured and ferritchromite is produced along the later cracks.

4.2. Listvenite

Listvenite (samples TDSL-11, TDSL-16, and TDSL-20) have a mineral assemblage consisting mainly of magnesite, talc, quartz, with a minor amount of antigorite, chlorite, magnetite, and relict chromian spinel (Figure 4(d,e)). Electron microprobe observations confirm the presence of tiny anthophyllite. Listvenite is schistose, with a penetrative schistosity defined by the preferred orientation of talc. Carbonate minerals (mainly magnesite) are often porphyroblastic and also occur as veins cross-cutting the matrix. Chromian spinel in listvenite occurs as subhedral grains, resembling that in the serpentinite; relict grains are fractured, overprinted by the ferritchromite along the later cracks (Figure 4(f)).

5. Bulk-rock chemistry

5.1. Serpentinite

Serpentinites (TDB-1, TDSD-4, TDSD-15, and TDSCH-18) are characterized by low contents of Al_2O_3 and CaO; the Al_2O_3 + CaO values range from 0.09 to 0.48 wt.% (normalized total as 100%). Serpentinization might have modified

Table 2. Representative electron microprobe analyses of olivine and relict chromian spinel.

Rock-type	Massive serpentinite					Schistose serp.		Listvenite		
Sample	TDSD15	TDSD15-2	TDSD4-2	TDSD15	TDSD15-2	TDB1	TDSCH18	TDSL11	TDSL16	TDSL16-2
Mineral	r.Ol	r.Ol	m.Ol	r.CrSp	r.CrSp	r.CrSp	r.CrSp	r.CrSp	r.CrSp	r.CrSp
Major-element compositions (in wt%)										
SiO_2	41.27	40.88	42.27							
TiO_2						0.04	0.03	0.03	0.03	
Cr_2O_3				60.11	61.91	61.66	60.52	63.77	56.82	62.21
Al_2O_3				6.81	6.21	6.04	7.55	6.92	10.49	6.80
FeO*	8.88	8.44	4.2	27.45	26.11	25.17	24.96	20.97	16.82	19.88
MnO	0.15	0.14	0.13	0.27	0.43	0.60	0.44	0.26	0.22	0.32
MgO	49.36	49.19	52.94	4.41	5.27	6.00	6.38	8.92	15.23	9.47
CaO	0.02	0.00	0.03							
NiO	0.42	0.45	0.3							
Total	100.10	99.10	99.87	99.05	99.93	99.51	99.88	100.87	99.61	98.68
O=4										
Si	1.006	1.005	1.010							
Ti						0.001	0.001	0.010	0.010	
Cr				1.670	1.700	1.690	1.640	1.680	1.430	1.700
Al				0.280	0.250	0.250	0.310	0.270	0.390	0.270
Fe^{3+}				0.030	0.030	0.040	0.040	0.030	0.110	0.050
Fe^{2+}	0.181	0.170	0.084	0.770	0.720	0.690	0.670	0.560	0.340	0.520
Mn	0.003	0.003	0.003	0.010	0.010	0.020	0.010	0.010	0.010	0.010
Mg	1.794	1.800	1.886	0.230	0.270	0.310	0.330	0.440	0.720	0.480
Ca	0.000	0.000	0.001							
Ni	0.008	0.009	0.006							
Total	2.992	2.987	2.990	2.99	2.98	3.00	3.00	3.00	3.01	3.03
Fo	90.8	91.4	95.7							
Mg#				0.23	0.27	0.31	0.33	0.44	0.68	0.48
Cr#				0.86	0.87	0.87	0.84	0.86	0.79	0.86

*Total Fe as FeO; r.Ol, relict olivine; m.Ol, metamorphic olivine; r.CrSp, relict chromian spinel
Fo, forsterite (mole%) in olivine; Mg#, Mg(Mg+Fe2+) atomic ratio of rCrSp; Cr#—Cr/(Cr+Al) atomic ratio of r.CrSp

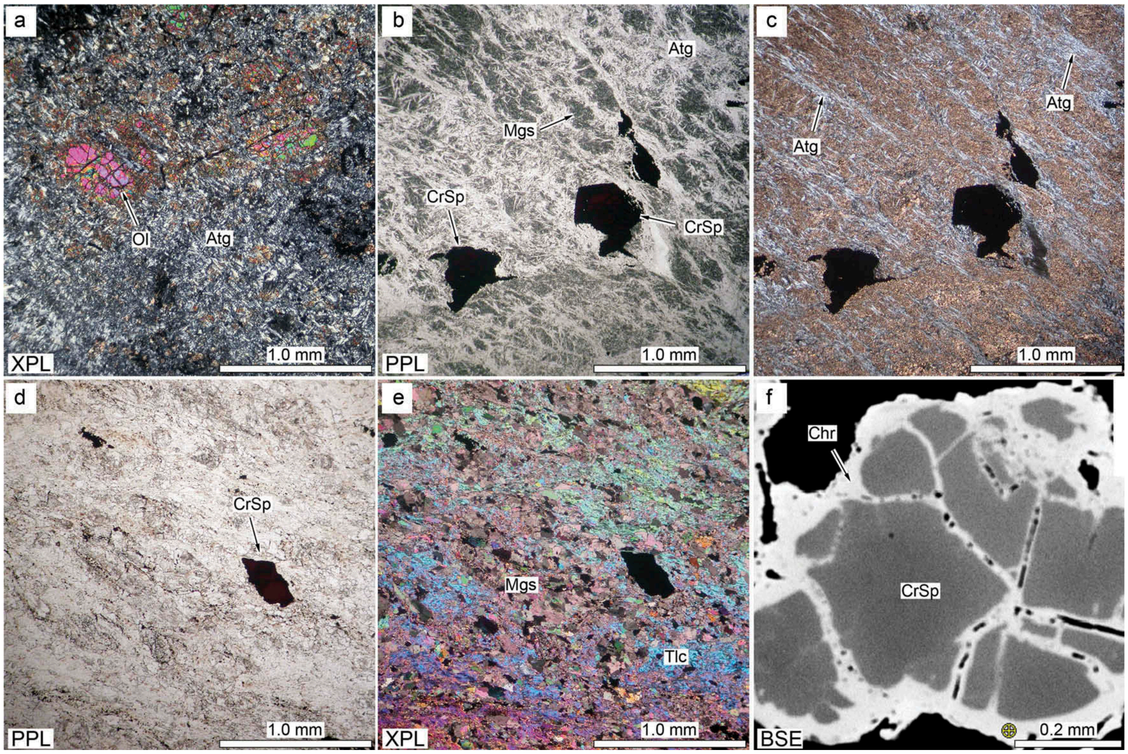

Figure 4. Micro-textures of serpentinites and listvenite from the Tulu Dimtu. (a) Crossed-polar light (XPL) view of a massive serpentinite, preserving relict olivine. (b) Plane-polar light (PPL) view of relict chromian spinel in a schistose serpentinite. (c) XPL view of (b); antigorites show a preferred orientation. (d) PPL view of relict chromian spinel in a listvenite. (e) XPL view of (d). (f) Back-scattered electron (BSE) image of zoned chromian spinel. Mineral abbreviations: Atg: antigorite; Chr: ferritchromite; CrSp: chromian spinel; Mgs: magnesite; Tlc: talc.

the original bulk-rock composition, particularly the strong depletion of CaO. The concentrations of Ni and Cr in samples TDB-1 and TDSCH-18 reach up to ~8923 µg/g and ~2446 µg/g, respectively. Bulk-rock Mg# [=Mg/(Mg+Fe^{2+}) atomic ratios] is 0.89–0.91. Serpentinites are characterized by extremely low abundances of incompatible trace elements (e.g. Ti, Ba, Nb, Sr, Y, and Zr). The concentrations of Al_2O_3, CaO, Cr, and Ni roughly correlate with MgO. The bulk-rock loss on ignition (LOI) values are in the range of 11.5–23.9 wt.% (Table 1). No significant differences in chemical composition among massive and schistose serpentinites were found.

5.2. Listvenite

Listvenite (TDSL-11, TDSL-16, and TDSL-20) is characterized by low SiO_2 (31.4–36.5 wt.%) and MgO (35.0–36.2 wt.%) contents, but has relatively higher LOI values up to ~20–23 wt.%. One sample of listvenite (TDSL-20) contains slightly higher Al_2O_3 (0.35 wt.%) compared with that in other samples (<0.24 wt.% Al_2O_3) (Table 1). The concentrations of Cr and Ni in listvenite resemble those of serpentinites. Similarly, listvenites are also depleted in Ti, Ba, Nb, Sr, Y, and Zr with a slight variation (Table 1).

6. Mineral composition

6.1. Chromian spinel

The chemical composition of chromian spinels is plotted in Cr–Al–Fe^{3+} ternary and Cr#–Mg# diagrams (Figures 5 and 6(a)). Chromian spinels in serpentinites are zoned. The cores are characterized by high Cr/(Cr+Al) atomic ratio (Cr# = 0.78–0.89), moderate to low Mg/(Mg+Fe^{2+}) atomic ratio (Mg# = 0.21–0.48), and very low Fe^{3+}/(Fe^{3+}+Cr+Al) atomic ratio (Fe^{3+}#<0.02) (Figure 6). They contain low TiO_2 (<0.1 wt.%) and MnO (<0.7 wt.%). The rims are highly oxidized and replaced by ferritchromite (and/or Cr-bearing magnetite). They are characterized by a high but wide range of Fe^{3+}# (~0.2–0.99) and low Mg# (0.19–0.35).

Chromian spinels in listvenite are relatively magnesian, Mg# = 0.38–0.65. Cr# ranges from 0.78 to 0.88, with very low Fe^{3+}# (<0.02) and low TiO_2 (<0.01 wt.%).

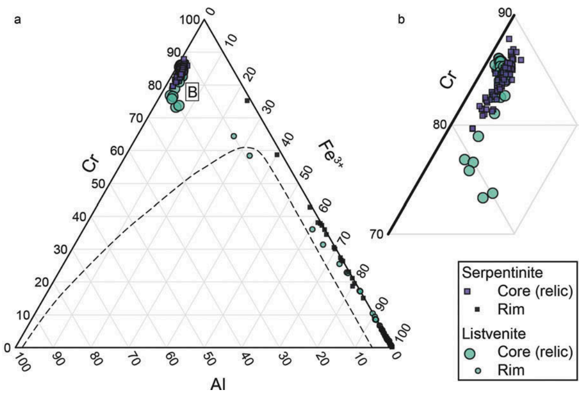

Figure 5. (a) Cr–Al–Fe^{3+} ternary diagram showing compositional variations of chromian spinels and ferritchromite from serpentinites and listvenite. Dashed line represents a solvus at 600°C proposed by Loferski and Lipin (1983). (b) Enlarged region in (a) for a comparison between relict chromian spinel among serpentinites and listvenite.

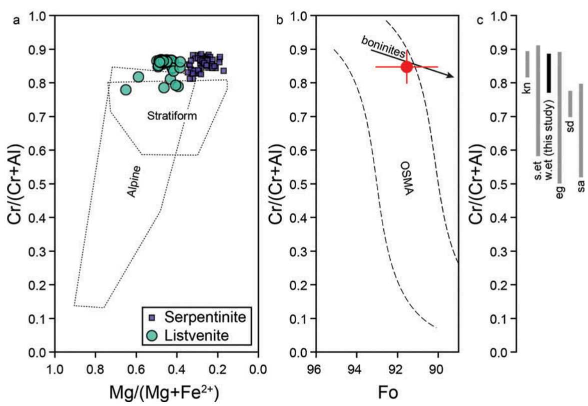

Figure 6. (a) Cr#–Mg# diagram showing compositional variations of relict chromian spinels (core compositions of zoned chromian spinels) from serpentinites and listvenite; compositions of secondary ferritchromitite are not plotted. Generalized compositional ranges from the Alpine and stratiform peridotites by Evans and Frost (1975) are also shown for comparison. (b) Compositional relationship between relict olivine and chromian spinel. OSMA (olivine–spinel mantle array) and a fractionation line of boninites are after Arai (1994). Cross bars represent compositional variations. (c) Comparisons of Cr# of chromian spinel from various ophiolitic bodies of the Arabian–Nubian Shield. Abbreviations and references: kn, Kenya (Price 1984; Berhe 1988); s.et, Southern Ethiopia (Berhe 1988; Bonavia *et al*. 1993); w.et, Western Ethiopia (this study); eg, Egypt (Ahmed *et al*. 2001; Hamdy and Lebda 2011; Abu-Alam and Hamdy 2014); sd, Sudan (Price 1984; Abdel-Rahman 1993; Hussein 2000); sa, Saudi Arabia (Al-Shanti 1982; LeMetrour *et al*. 1982; Chevremont and Johan 1982a, 1982b; Ledru and Auge 1984; Al-Shanti and El-Mahdy 1988).

6.2. Olivine

In massive serpentinites, metamorphic olivines with tiny magnetites are high-magnesian, containing high forsterite [Fo] content (Fo_{93-96}) with variable NiO (0.19–0.52 wt.%) and MnO (0.02–0.19 wt.%) contents. In contrast, magnetite-free relict primary mantle olivine has a composition of Fo_{90-93} with 0.25–0.49 wt.% NiO and ~0.08–0.22 wt.% MnO; this is comparable to typical mantle olivine. The relationship between the Fo content of the relict olivine (Fo_{90-93}) and the cores of chromian spinel (Cr# = 0.78–0.89) in massive serpentinite suggests a spinel-bearing, highly depleted harzburgite as the original mantle peridotite (Figures 6B) (Arai 1994).

7. Discussion

7.1. Tectonic setting of the Tulu Dimtu ultramafic bodies

The inferred original peridotite, with a chromian spinel of Cr# = 0.78–0.89 and a relict olivine of Fo_{90-93}, is a highly depleted residual harzburgite. This is a robust evidence that the peridotite formed in an environment with a very high degree of melt depletion, likely formed in a suprasubduction zone wedge mantle (e.g. Dick and Bullen 1984; Ishiwatari 1985; Arai 1994; Arai and Yurimoto 1994, 1995; Bloomer *et al*. 1995; Zhou *et al*. 1998; Dilek and Flower 2003). As shown in Figure 6(b), the compositional relationship between relict olivine and chromian spinel overlaps with a fractionation line of boninites.

The ultramafic rocks of the Tulu Dimtu can be compared to serpentinized residual spinel-harzburgites of the ANS ophiolite (e.g. Stern *et al*. 2004); Cr# value of the chromian spinel of Tulu Dimtu overlaps with the variations of most ANS ophiolite bodies, such as South Ethiopia, Kenya, Sudan, and Egypt (Figure 6(c)). As previously thought in the ANS ophiolite, we interpret that the ultramafic rocks of Tulu Dimtu formed in suprasubduction zone settings.

7.2. Conditions of listvenite formation and later regional metamorphism

The occurrence of relict chromian spinel in listvenite suggests an inevitable petrogenetic relationship between listvenite and associated ultramafic rocks. In fact, listvenites are closely associated with smaller ultramafic lenses, suggesting they formed by a metasomatic replacement of smaller ultramafic lenses within metasedimentary mélange.

It has been considered that listvenite formed at low pressure and low temperature (e.g. Falk and Kelemen 2015). Tsikouras *et al*. (2006) considered the external influx of SiO_2 via low-pH, highly oxidized, saline-rich, low-temperature (T < ~250°C) fluids. On the other hand, Hansen *et al*. (2005) proposed the direct transformation of mantle peridotite to listvenite from the following reactions:

$$34\ Mg_2SiO_4[\text{olivine}] + 20\ CO_2 + 31\ H_2O = Mg_{48}Si_{34}O_{85}(OH)_{62}[\text{antigorite}] + 20\ MgCO_3[\text{magnesite}]$$

$$2\ Mg_{48}Si_{34}O_{85}(OH)_{62}[\text{antigorite}] + 45\ CO_2 = 45\ MgCO_3[\text{magnesite}] + 17\ Mg_3Si_4O_{10}(OH)_2[\text{talc}] + 45\ H_2O$$

$$Mg_3Si_4O_{10}(OH)_2[\text{talc}] + 3\ CO_2 = 3MgCO_3[\text{magnesite}] + 4\ SiO_2[\text{quartz}] + H_2O$$

These reactions occur at a nearly constant MgO:SiO_2 ratio, except for the addition of water and CO_2 during listvenite formation. In the investigated listvenite, MgO and SiO_2 underwent a little depletion, as compared with those in the serpentinites. However, the apparent depletion is attributed to the addition of a large volume of CO_2, as suggested by Hansen *et al*. (2005). Recently Falk and Kelemen (2015) studied listvenite veins from the Samail ophiolite (Oman) and confirmed the low-temperature (~100°C) formation of listvenite using oxygen isotope thermometry. In Tulu Dimtu, listvenite-forming metasomatism was probably initiated by low-temperature conditions. However, metasedimentary mélange including serpentinites and listvenite has suffered the later amphibolite-facies regional metamorphism of the ANS; both serpentinite and listvenite were deformed during the metamorphism.

The presence of antigorite and talc in the assemblage of listvenite suggests that listvenite was recrystallized at a temperature of over 300–400°C. A finding of anthophyllite in listvenite suggests that the temperature conditions reached up to 500–550°C at a nominal pressure of 0.6–0.7 GPa (Ford and Skippen 1997). The mineral assemblage antigorite + metamorphic olivine ± talc in massive serpentinite indicates that the ultramafic rocks suffered a regional metamorphism under conditions of $T = \sim 350$–550°C (e.g. Evans 2010). According to a petrogenetic grid for carbonate-bearing hydrous ultramafic rocks by Will *et al*. (1990), this metamorphic temperature is consistent with the mineral assemblage metamorphic olivine + magnesite + talc ± chlorite in massive serpentinite.

7.3. Relative timing of listvenite formation

As we described, listvenite in Tulu Dimtu contains relict chromian spinel that overlaps the Cr# with those observed in serpentinites. However, relict chromian spinel in the listvenite has a significantly higher Mg# value (Figure 6(a)). In general, equilibrium temperatures of mantle minerals in peridotites or serpentinized peridotites are controlled by cooling history (e.g. Arai 1980). If ultramafic rocks cool at a slow rate, highly resistant minerals like chromian spinel can continue to re-equilibrate until the closing temperature of sub-solidus Mg–Fe^{2+} redistribution among the surrounding mafic minerals such as olivine and serpentine. Hence we interpret that the listvenite formation, that is, a nealy complete metasomatic replacement of silicate minerals in primary ultramafic rocks, would be an earlier event of the Tulu Dimtu ultramafic rocks and was not related to the late metamorphic process of the ANS.

Based on our petrological observation together with the geological context, we propose the following geological scenario (Figure 7). (1) The Tulu Dimtu ultramafic rocks that formed in a suprasubduction zone setting were tectonically emplaced within a calcareous sedimentary mélange of an accretionary prism developed along

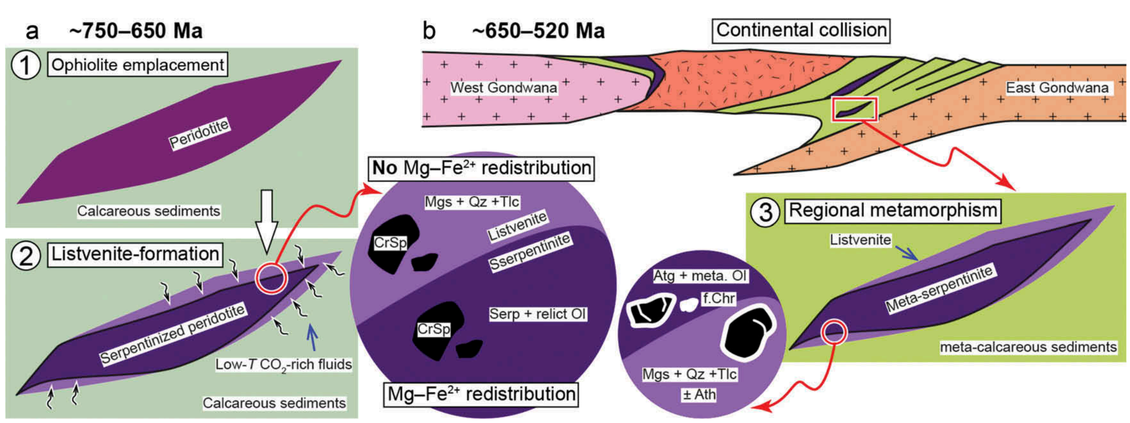

Figure 7. Schematic model of listvenite formation (see the details in text); approximate time intervals are based on a regional geological context. (a) Ophiolite emplacement: a tectonic emplacement of suprasubduction zone mantle peridotite – (Process 1) and listvenite formation in calcareous sediments (Process 2) at ~750–650 Ma. A nearly complete metasomatic replacement of ultramafic rocks by magnesite, talc, and quartz prevented Mg–Fe^{2+} redistribution between relict chromian spinel and the host. (b) Regional metamorphism of the Arabian–Nubian Shield (Process 3) at ~650–520 Ma. The metamorphism involves deformation to have formed schistosity in both listvenite and serpentinite.

the west Gondwana margin, probably at ~750–650 Ma. (2) The ultramafic sheets or lenses interacted with host calcareous sedimentary rocks; during this process, low-temperature CO_2-rich hydrothermal fluids infiltrated into ultramafic rocks and erased the minerals except for chromian spinel. Mg# of chromian spinel was frozen due to the loss of equilibrating mafic minerals in listvenite. In ultramafic rocks with partial carbonate metasomatism, Mg# in chromian spinel was continuously changed due to sub-solidus Mg–Fe^{2+} redistribution. (3) Regional metamorphism due to the continental collision of Gondwana amalgamation took place at ~650–520 Ma; the so-called 'Pan-African' metamorphic event formed metamorphic olivine and rare anthophyllite in serpentinites. The oxidation of relict chromian spinel to form ferritchromite and/or Cr-bearing magnetite occurred both in serpentinite and in listvenite during this stage.

Origin and source of CO_2-rich hydrothermal fluids remain to be constrained. To further our understanding of listvenite, a detailed and comprehensive approach to geology, petrology, and geochronology is required.

Acknowledgements

We dedicate this paper to Dr Sorena S. Sorensen who has addressed the significance of metasomatism associated with serpentinite. This work was supported by Tohoku University in part by the Takuetsu Program and the Japanese Government MEXT Scholarship awarded to Sofiya and MEXT/JSPS KAKENHI (15H05212) to Tsujimori. We thank H.U. Rehman and K.E. Flores who have critically reviewed this manuscript and W.G. Ernst and R.J. Stern for constructive editorial evaluation. We also thank S. Machi, D. Ayalew, and members of the Petrotectonics Research Group for their assistance in laboratory work and helpful discussion.

Disclosure statement

No potential conflict of interest was reported by the authors.

Funding

This research was supported in part by MEXT/JSPS KAKENHI to Tsujimori [15H05212].

ORCID

Ayano Sofiya http://orcid.org/0000-0002-3124-9680
Naoto Hirano http://orcid.org/0000-0003-3491-0312
Tatsuki Tsujimori http://orcid.org/0000-0001-9202-7312

References

Abdel-Rahman, M., 1993, Geochemical and geotectonic controls of the metallogenic evolution of selected ophiolite complexes from the Sudan: Berliner Geowissenschaftliche Abhandlungen, v. 145, p. 175.

Abdelsalam, M.G., and Stern, R.J., 1996, Sutures and shear zones in the Arabian-Nubian Shield: Journal of African Earth Sciences, v. 23, p. 289–310. doi:10.1016/S0899-5362(97)00003-1

Abu-Alam, T.S., and Hamdy, M.M., 2014, Thermodynamic modelling of Sol Hamed serpentinite, South Eastern Desert of Egypt: Implication for fluid interaction in the Arabian–Nubian Shield ophiolites: Journal of African Earth Sciences, v. 99, p. 7–23. doi:10.1016/j.jafrearsci.2014.06.001

Aftabi, A., and Zarrinkoub, M.H., 2013, Petrogeochemistry of listvenite association in metaophiolites of Sahlabad region, eastern Iran: Implications for possible epigenetic Cu-Au ore exploration in metaophiolites: Lithos, v. 156–159, p. 186–203. doi:10.1016/j.lithos.2012.11.006

Ahmed, A.H., Arai, S., and Attia, A.K., 2001, Petrological characteristics of podiform chromitites and associated peridotites of the Pan African Proterozoic ophiolite complexes of Egypt: Mineralium Deposita, v. 36, p. 72–84. doi:10.1007/s001260050287

Alemu, T., and Abebe, T., 2000, Geology of the Gimbi area: Geological Survey of Ethiopia, Memoir 15, Addis Ababa, Ethiopia, Geological Survey of Ethiopia, 158 p.

Al-Shanti, A.M., and El-Mahdy, O.R., 1988, Geological studies and assessment of chromite occurrences in Saudi Arabia: KACST Project No. AT-6-094.

Al-Shanti, M.M.S., 1982, Geology and mineralization of the Ash Shizm-Jabal Ess area [Ph.D. thesis]: King Abdulaziz University, 291 p.

Arai, S., 1980, Dunite-harzburgite-chromitite complexes as refractory residue in the Sangun-Yamaguchi zone, western Japan: Journal of Petroleum, v. 21, p. 141–165.

Arai, S., 1994, Characterization of spinel peridotites by olivine-spinel compositional relationships: Review and interpretation: Chemical Geology, v. 113, p. 191–204.

Arai, S., and Yurimoto, H., 1994, Podiform chromitites of the Tari-Misaka ultramafic complex, Southwestern Japan, as mantle–melt interaction products: Economic Geology, v. 89, p. 1279–1288. doi:10.2113/gsecongeo.89.6.1279

Arai, S., and Yurimoto, H., 1995, Possible sub-arc origin of podiform chromitites: The Island Arc, v. 4, p. 104–111. doi:10.1111/iar.1995.4.issue-2

Ayalew, T., Bell, K., Moore, J.M., and Parrish, R.R., 1989, The Gore Gambella Geotraverse, Western Ethiopia: Open file report, IDC, p. 153.

Ayalew, T., Bell, K., Moore, J.M., and Parrish, R.R., 1990, U-Pb and Rb-Sr geochronology of the Western Ethiopian Shield: Geological Society of America Bulletin, v. 102, p. 1309–1316. doi:10.1130/0016-7606(1990)102<1309:UPARSG>2.3.CO;2

Berhe, S.M., 1988, The geologic and tectonic evolution of the Pan African/Mozambique Belt in East Africa [Ph.D. thesis]: Milton Keynes, Open University, 265 p.

Bloomer, S.H., Taylor, B., MacLeod, C.J., Stern, R.J., Fryer, P., Hawkins, J.W., and Johanson, L., 1995, Early arc volcanism and the ophiolite problem: A perspective from drilling in the Western Pacific, *in* Taylor, B., and Natland, J., eds., Active

margins and marginal basins of the the Western Pacific: Washington, DC, American Geophysical union, p. 1–30.
Boedo, F.L., Escayola, M.P., Perezlujan, S.B., Vujovich, G.I., Ariza, J.P., and Naipauer, M., 2015, Geochemistry of Precordillera serpentinites, western Argentina: Evidence for multistage hydrothermal alteration and tectonic implications for the Neoproteroterozoic-Early Paleozoic: Geologica Acta, v. 13, p. 263–278.
Bonavia, F.F., Diella, V., and Ferrario, A., 1993, Precambrian podiform chromitites from Kenticha Hill, Southern Ethiopia: Economic Geology, v. 88, p. 198–202. doi:10.2113/gsecongeo.88.1.198
Chevremont, P., and Johan, Z., 1982a, The Al Ays ophiolite complex: BRGM-OF-02-5, Saudi Arabia Deputy Ministry for Mineral Resources.
Chevremont, P., and Johan, Z., 1982b, Wadi al Hwanet-Jabal Iss ophiolite complexe: BRGM-OF-02-14, Saudi Arabia Deputy Ministry for Mineral Resources.
De Wit, M.J., and Chewaka, S., 1981, Plate tectonic evolution of Ethiopia and mineral deposits: An overview, *in* Chewaka, S., and De Wit, M.J., eds., Plate Tectonics and Metallogenesis, Some Guide Lines to Ethiopian Mineral Deposits: Ethiopian Institute of Geological Surveys Bulletin, v. 2, p. 115–119.
Dick, H.J.B., and Bullen, T., 1984, Chromian spinel as a petrogenetic indicator in abyssal and alpine-type peridotites and spatially associated lavas: Contributions to Mineralogy and Petrology, v. 86, p. 54–76. doi:10.1007/BF00373711
Dilek, Y., and Flower, M.F.J., 2003, Arc-trench roll-back and forearc accretion: 2. A model template for ophiolites in Albania, Cyprus, and Oman, *in* Dilek, Y., and Robinson, P. T., eds., Ophiolites in Earth History: Geological Society of London Special Publication 218, p. 43–68.
Evans, B.W., 2010, Lizardite versus antigorite serpentinite: Magnetite, hydrogen, and life? Geology, v. 38, p. 879–882. doi:10.1130/G31158.1
Evans, B.W., and Frost, B.R., 1975, Chrome-spinel in progressive metamorphism: A preliminary analysis: Geochimica et Cosmochimica Acta, v. 39, p. 959–972. doi:10.1016/0016-7037(75)90041-1
Falk, E.S., and Kelemen, P.B., 2015, Geochemistry and petrology of listvenite in the Samail ophiolite, Sultanate of Oman: Complete carbonation of peridotite during ophiolite emplacement: Geochimica et Cosmochimica Acta, v. 160, p. 70–90. doi:10.1016/j.gca.2015.03.014
Ford, F.D., and Skippen, G.B., 1997, Petrology of the Flinton Creek metaperidotites: Enstatite-magnesite and anthophyllite-magnesite assemblages from the Grenville Province: Canadian Mineralogist, v. 35, p. 1221–1236.
Fritz, H., Abdelsalam, M., Ali, K.A., Bingen, B., Collins, A.S., Fowler, A.R., Ghebreab, W., Hauzenberger, C.A., Johnson, P. R., Kusky, T.M., Macey, P., Muhongo, S., Stern, R.J., and Viola, G., 2013, Orogen styles in the East African Orogen: A review of the Neoproterozoic to Cambrian tectonic evolution: Journal of African Earth Sciences, v. 86, p. 65–106. doi:10.1016/j.jafrearsci.2013.06.004
Grenne, T., Pederesen, R.B., Bjerkgard, T., Braathen, A., Selassie, M.G., and Worku, T., 2003, Neoproterozoic evolution of Western Ethiopia: Igneous geochemistry, isotope systematics and U–Pb ages: Geological Magazine, v. 140, p. 373–395. doi:10.1017/S001675680300801X
Halls, C., and Zhao, R., 1995, Listvenite and related rocks: Perspectives on terminology and mineralogy with reference to an occurrence at Cregganbaun, Co. Mayo, Republic of Ireland: Mineralium Deposita, v. 30, p. 303–313. doi:10.1007/BF00196366
Hamdy, M.M., and Lebda, E.M., 2011, Al-compositional variation in ophiolitic chromitites from the south Eastern Desert of Egypt; petrogenetic implications: Journal of Geology and Mining Research, v. 9, p. 232–250.
Hansen, L.D., Dipple, G.M., Gordon, T.M., and Kellett, D.A., 2005, Carbonated serpentinite (listwanite) at Atlin, British Columbia: A geological analogue to carbon dioxide sequestration: The Canadian Mineralogist, v. 43, p. 225–239. doi:10.2113/gscanmin.43.1.225
Harlow, G.E., Tsujimori, T., and Sorensen, S.S., 2015, Jadeitites and plate tectonics: Annual Review of Earth and Planetary Sciences, v. 43, p. 105–138. doi:10.1146/annurev-earth-060614-105215
Hussein, I.M., 2000, Geodynamic evolution of the Pan-African crystalline basement in the northern Red Sea Hills, Sudan, with special emphasis on the Wadi Onib ophiolite and geology to the west of Port Sudan: Mainz, Joahnnes Gutenberg Universität-Mainz.
Ishiwatari, A., 1985, Igneous petrogenesis of the Yakuno ophiolite (Japan) in the context of the diversity of ophiolites: Contributions to Mineralogy and Petrology, v. 89, p. 155–167.
Kazmin, V., 1972, Geology of Ethiopia: Unpublished report, Ethiopian institute of Geological Surveys.
Kazmin, V., 1976, Ophiolite in the Ethiopian basement: Ethiopian Institute of Geological Surveys.
Kazmin, V., Shiferaw, A., Tefera, M., Berhe, S.M., and Chewaka, S., 1978, The Ethiopian basement: Stratigraphy and possible manner of evolution: Geologische Rundschau, v. 67, p. 531–546. doi:10.1007/BF01802803
Kebede, T., Koeberl, C., and Koller, F., 1999, Geology, geochemistry and petrogenesis of intrusive rocks of the Wallagga area, western Ethiopia: Journal of African Earth Sciences, v. 29, p. 715–734. doi:10.1016/S0899-5362(99)00126-8
Kebede, T., Koeberl, C., and Koller, F., 2001, Magmatic evolution of the suqii-wagga garnet-bearing two-mica granite, wallagga area, western Ethiopia: Journal of African Earth Sciences, v. 32, p. 193–221. doi:10.1016/S0899-5362(01)90004-1
Kröner, A., 1984, Late Precambrian plate tectonics and orogeny: A need to redefine the term Pan-African, *in* Klerkx, J., and Michot, J., eds., African geology: Tervuren, Mu'ee R. L' Afrique Centrale, p. 23–28.
Ledru, P., and Auge, T., 1984, The Al Ays ophiolitic complex; petrology and structural evolution: BRGM-OF-04-15, Saudi Arabia Deputy Ministry for Mineral Resources.
LeMetrour, J., Johan, V., and Tegyey, M., 1982, Relationships between ultramafic-mafic complexes and volcanosedimentary rocks in the Precambrian Arabian Shield: BRGM-OF-02-15, Saudi Arabia Deputy Ministry for Mineral Resources.
Loferski, P.J., and Lipin, B.R., 1983, Exsolution in metamorphosed chromite from Red Lodge district, Montana: American Mineralogist, v. 68, p. 777–789.
Price, R.C., 1984, Late Precambrian Mafic-Ultramafic Complexes in Northeast Africa [Ph.D. thesis]: Milton Keynes, Open University, 325 p.
Sorensen, S.S., Sisson, V.B., Harlow, G.E., and AvéLallemant, H. G., 2010, Element residence and transport during subduction-zone metasomatism: Evidence from a jadeitite-serpentinite contact, Guatemala: International Geology Review, v. 52, p. 899–940. doi:10.1080/00206810903211963

Stern, R.J., 1993, Tectonic evolution of the late Proterozoic East African Orogen: Constraints from crustal evolution in the Arabian-Nubian Shield and the Mozambique Belt, *in* Thorweihe, U., and Schandelmeier, H., eds, Geoscientistific Research in Northeast Africa: p. 73–74.

Stern, R.J., 1994, Arc assembly and continental collision in the Neoproterozoic East African Orogen: Implications for the consolidation of Gondwanaland: Annual Review of Earth and Planetary Sciences, v. 22, p. 319–351. doi:10.1146/annurev.ea.22.050194.001535

Stern, R.J., Johnson, P.R., Kroner, A., and Yibas, B., 2004, Neoprotrozoic ophiolites of the Arabian-Nubian Shield, *in* Kusky, T.M., ed., Precambrian Ophiolites and Related Rocks, Amsterdam: Elsevier, Developments in Precambrian Geology: v. 13, p. 95–128.

Tadesse, A., and Tsegaye, A., 2007, Geology and Tectonic evolution of the Pan-African Tulu-Dimtu Belt, Western Ethiopia: Journal of Earth Science, v. 1, p. 24–42.

Tadesse, G., and Allen, A., 2005, Geology and geochemistry of the Neoproterozoic Tuludimtu Ophiolite suite, western Ethiopia: Journal of African Earth Sciences, v. 41, p. 192–211. doi:10.1016/j.jafrearsci.2005.04.001

Tefera, M., Cherenet, T., and Haro, W., 1996, Geological map of Gore area (1:2000, 000): Ethiopian Institute of Geological Surveys.

Tsikouras, B., Karipi, S., Grammatikopoulos, T.A., and Hatzipanagiotou, K., 2006, Listwaenite evolution in the ophiolite mélange of Iti Mountain (continental Central Greece): European Journal of Mineralogy, v. 18, p. 243–255. doi:10.1127/0935-1221/2006/0018-0243

Will, T.M., Powell, R., and Holland, T.J.B., 1990, A calculated petrogenetic grid for ultramafic rocks in the system CaO-FeO-MgO-Al_2O_3-SiO_2-CO_2-H_2O at low pressures: Contributions to Mineralogy and Petrology, v. 105, p. 347–358. doi:10.1007/BF00306544

Zhou, M.F., Sun, M., Keays, R.R., and Kerrich, R.W., 1998, Controls on platinum-group elemental distributions of podiform chromitites: A case study of high Cr and high-Al chromitites from Chinese orogenic belts: Geochimica et Cosmochimica Acta, v. 62, p. 677–688. doi:10.1016/S0016-7037(97)00382-7